Journal of Applied Biological Sciences 3(2): 85-91, 2009
ISSN: 1307-1130, www.nobel.gen.tr

Adsorption of Pb (II) Ions by *Lemma minor, Potamogeton crispus* and *Chara vulgaris*: Kinetic Modelling

Osman GULNAZ

Department of Science and Technology Education, Cukurova University, 01330 Balcalı, Adana, TURKEY

***Corresponding Author**
e-mail: ogulnaz@mail.yahoo.com

Received: April 25, 2009
Accepted: June 07, 2009

ABSTRACT

In this study, adsorption of Pb (II) ions by aquatic macrophte *Lemma minor*, *Potamogeton crispus* and *Chara vulgaris*. The effects of pH, initial metal concentration on adsorption were determined. The optimum adsorption pH was determined to be 4 for *L. minor* and *P. crispus* and pH 5 for *C. vulgaris*. Maximum adsorption capacities of adsorbents were determined to be 93.4, 88.4 and 64 mgg^{-1} for *L. minor*, *P. crispus* and *C. vulgaris*, respectively. Adsorption efficiency was observed in the order of *L. minor* > *P. crispus* > *C. vulgaris* for removal of Pb (II) ions.

The adsorption kinetics were also found to be well-described by the pseudo second-order and intra-particle diffusion models. *L. minor*, *P. crispus* and *C. vulgaris* have different functional groups, which include carboxyl (-COOH), phosphate ($-PO_4$), amide ($-NH_2$), and hydroxide (-OH) groups. These functional groups are able to react with heavy metal ions in aqueous solution.

Key Words: Lemma minor, Potamogeton crispus, Chara vulgaris, Adsorption, Kinetic models, Lead ions To whom correspondence should be directed,

INTRODUCTION

The increase in toxic metal contamination is an important environmental problem. Heavy metals are toxic even at low concentrations. The main sources of heavy metals are wastewaters from processes such as electroplating, battery manufacturing, automotive manufacturing, metal finishing, mining, and steelwork.

Many physicochemical techniques such as chemical coagulation, extraction, ion exchange, membrane separation, and electrochemistry have been used to remove heavy metal from wastewater [1-3]. But, these techniques have significant disadvantages including incomplete metal removal, expensive equipment and energy requirements or generation of toxic sludge [2-5].

Adsorption is an alternative technique for the removal of pollutants from aqueous solutions. Activated carbon is the most common commercial adsorbent material but it is a very expensive, for this reason, many researchers focus on the feasibility of identifying an inexpensive adsorbent. Many adsorbent materials such as seaweeds, algae, yeast, fungi, activated sludge, sawdust [1-8].

Lead widely used toxic industrial chemicals. The main objective of this article is the removal of Pb (II) from aqueous solution via adsorption through the use and re-use of aquatic macrophte *L. minor*, *P. crispus* and *C. vulgaris*. The effects of pH and initial metal concentration on adsorption were determined. Adsorbents was characterized by using Frouier Transformation Infrared Spectrophotometer (FT-IR). The Langmuir adsorption isotherm model and pseudo-first, pseudo-second order and intraparticle diffusion models were used to determine the adsorption isotherm and kinetics.

Theoretical

The Langmuir adsorption isotherm model is a widely used theoretical model for describing the adsorption isotherm [9]. The linear Langmuir equation is:

$$\frac{C_e}{q_e} = \frac{1}{k_L} + \left(\frac{a_L}{k_L}\right)C_e$$
(1)

where, a_L and k_L are the Langmuir isotherm constants and the ratio of k_L / a_L gives the theoretical monolayer saturation capacity of biomass ($q_{\max}$). The essential characteristic of the Langmuir equation can be expressed in terms of dimension factor R_L, which was defined by Hall et al., [10] as:

$$R_L = \frac{1}{1 + K_L C_0}$$
(2)

where, K_L is the Langmuir isotherm constant and C_0 is the highest initial metal concentration (mgL^{-1}). The value of R_L indicates the shape of the isotherms to be either unfavourable (R_L >1), linear (R_L =1), favourable (0< R_L <1) or irreversible (R_L =0).

The pseudo first-order [11] , pseudo second-order [12] and intraparticle diffusion model [13] were used to describe adsorption kinetics.

The pseudo first-order model:

$$Log(q_e - q_t) = Logq_e - \frac{k_1}{2.303}t$$
(3)

The pseudo second-order model:

$$\frac{t}{q_t} = \frac{1}{k_2 q_e^2} + \frac{1}{q_e}t$$
(4)

The intraparticle diffusion model:

$$q_t = k_i t^{0,5} + C$$
(5)

where k_1 is the rate constant of pseudo first-order model (min^{-1}), k_2 (gmg^{-1}min) is the rate constant of pseudo second-order model, and k_i is the intraparticle diffusion rate constant (mgg^{-1}min$^{0.5}$). q_e and q_t are the amounts of metal adsorbed on the adsorbent (mgg^{-1}) at equilibrium and at time t, respectively.

MATERIALS AND METHODS

Biomass preparation and adsorption studies

Aquatic macrophtes *L. minor*, *P. crispus* and *C. vulgaris* biomass were obtained from Seyhan River, Adana-Turkey. The biomasses were washed twice with distilled water. It was dried at 60°C until a constant weight was obtained (96 h). Dried biomass was broken into pieces, which were separated into certain particle sizes (0.1-0.5mm), by a sieve.

Adsorption study was performed as previously described method [2,4]. A known amount of biosorbent (1 gL^{-1}) was combined with 500 mL of a known amount of Lead ions in 1000 mL screw top flasks, which were agitated on a shaker at 150 rpm to ensure equilibrium . Unadsorbed heavy metal ions were determined using an atomic absorption spectrophotometer (AAS). Before AAS analyses, samples were filtered with nylon membrane filters (0.45 µm). FT-IR analysis of biomasses was performed. The Perkin Elmer spectrum RX/FT-IR system was used for analysis of a KBr pellet (1/100 Biomass/KBr) [2,4].

The adsorption isotherm was studied at 20°C. The effect of the pH on adsorption was studied at pH values between 3 and 6. Effect of initial metal concentrations was determined at 50 and 100 mgL^{-1} Pb (II) concentrations . The solution pH was adjusted by H_2SO_4 or NaOH and was not controlled after the initial adjustment.

Metal uptake (q_e) was calculated using the following equation:

$$q_e = \frac{(C_0 - C_t)V}{1000W}$$
(6)

where q_e (mgg^{-1}) is the amount of total adsorbed heavy metal ions, C_0 (mgL^{-1}) is the initial metal concentration, C_t (mgg^{-1}) is the equilibrium metal concentration in solution at time t, V (L) is the solution volume and W (g) is the adsorbent weight.

Control samples were prepared from the biomass free solution for testing metal losses due to metal precipitation and adsorption to the bottle surface. All experiments were performed at least in duplicate. Results shown are the means of the duplicate experimental results.

RESULTS AND DISCUSSION

FT-IR analysis of dried biomass

Aquatic macrophytes, *L. minor*, *P. crispus* and *C. vulgaris*, consists of complex organic and inorganic materials such as proteins, lipids, carbohydrate polymers, Ca^{+2}, Mg^{+2}, etc. The FT-IR spectrum and characteristic bands of *L. minor*, *P. crispus* and *C. vulgaris* are given in Table 1.

Table 1. Characteristic FT-IR spectral region bands of aquatic macrophtes

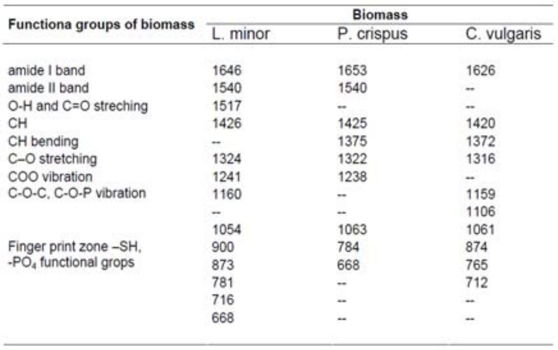

Functiona groups of biomass	Biomass		
	L. minor	P. crispus	C. vulgaris
amide I band	1646	1653	1626
amide II band	1540	1540	--
O-H and C=O streching	1517	--	--
CH	1426	1425	1420
CH bending	--	1375	1372
C–O stretching	1324	1322	1316
COO vibration	1241	1238	--
C-O-C, C-O-P vibration	1160	--	1159
	--	--	1106
	1054	1063	1061
Finger print zone –SH, -PO_4 functional grops	900	784	874
	873	668	765
	781	--	712
	716	--	--
	668	--	--

The band at 1646cm^{-1} band represents the stretching vibration of COO, C=O and C-N (amide I) protein peptide bonds. The 1540 cm^{-1} band represents the stretching vibration of C-N of protein peptide bonds. The 1238 cm^{-1} band is the vibration of carboxylic acids and stretching OH vibration phenolics. The 1160-1000 cm^{-1} band is the vibration of the C-O-C and OH of polysaccharides. The 873 cm^{-1} band represents a Si-H bend. <800 cm $^{-1}$ is the finger print zone, which represents phosphate and sulphur functional groups.

The carboxyl (-COOH), phosphate (-PO_4), amide (-NH_2) and hydroxide (-OH) groups of biomasses are able to react with cationic metal ions These functional groups are able to react with cationic metal ions [2,4]. The adsorption mechanism of Pb (II) probably occurs via ion exchange, surface complexation and electrostatic interaction between functional groups and free metal ions in solutions.

Effect of pH

The pH of solutions affects metal-biomass interaction, solubility of the metal ions and the charge of the functional end groups of the biomass, so pH is arguably the most important parameter for adsorption processes. Adsorption of metal ions correlated with the net negative charge of biomasses. Moreover, the net negative charge of the biomass in the solution was changed by solution pH. For this reason, the initial pH affects the adsorption capacity of adsorbent [14].

The adsorption capacity of *L. minor*, *P. crispus* and *C. vulgaris* increased with increasing pH from 3.0 to 6.0. The lowest metal uptake values were determined at low pH. Active groups of biomasses surface become protonated at lower pH and, in addition, the metal ions compete with the H^+ in the solution that is present at low pH values. Adsorption of heavy metal ions is mainly due to the ionic attraction between the biomass and metal ions [16].

The overall surface charge of the *L. minor*, *P. crispus* and *C. vulgaris* at lower pH values will be positive, which inhibits its interaction with positively charged metal cations [15]. In this study, the optimum pH was determined to be 4 for *L. minor*, *P. crispus* and 5 for *C. vulgaris*. The adsorption capacity of *L. minor*, *P. crispus* and *C. vulgaris* were determined to be 83, 78 and 56 mgg^{-1}, respectively. The mechanism of adsorption is probably the metal ion chelating with the functional groups of biomasses. The method of sorption is possibly ion exchange of the metal ion with the hydrogen ions protonating the functional end groups [17].

Effect of initial metal concentration and contact time

Many physicochemical factors, initial metal concentrations, ionic species, and the active site of the biosorbent, affect the adsorption capacity of an adsorbent. Effect of initial metal concentration on adsorption was studied at ion concentrations between 50 and 100 mgL^{-1} for Cd (II), Cu (II) and Pb (II) at 20°C. Results are given in Fig. 1. Equilibrium uptake increased with the increase in initial metal ion concentration from 50 to 100 mgL^{-1}. This occurs because the increase in metal ion concentration drives the concentration gradient toward higher adsorption. Under the same conditions, if the concentration of metal ions in solution was higher, the active sites of biomass would be surrounded by more metal ions and the process of adsorption would be more efficient. Therefore, the values of *qe* increased with increasing initial metal ion concentration [18]. The adsorption capacity of *L. minor*, *P. crispus* and *C. vulgaris* at a metal concentration of 50 mgL^{-1} was determined to be 47, 42 and 37 mgg $^{-1}$ at 50 mgL^{-1} initial metal concentrations, respectively. The adsorption capacity of *L. minor*, *P. crispus* and *C. vulgaris* at a metal concentration of 100 mgL^{-1} was determined to be 83, 78 and 56 mgg^{-1}, respectively. The equilibrium adsorption capacity of the biomass was increased with increasing initial metal concentration. Adsorption studies were carried out for 200 minutes in order to determine effect of contact time on adsorption. Most of the metal ions were adsorbed from aqueous solution within the first 15-20 minutes and almost no increase in the amount of biosorbed metal occurred after 180 minutes.

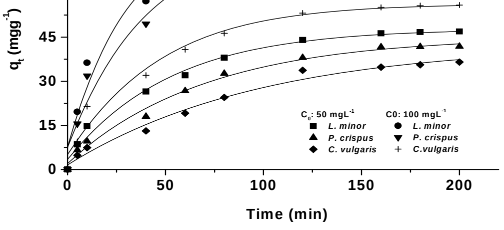

Fig. 1. Effect of initial metal concentrations on adsorption

Adsorption isotherm

The equilibrium adsorption isotherm is used to describe experimental sorption data. The Langmuir model is probably the best known and most widely applied sorption isotherm equation. Langmuir considered the adsorption of an ideal gas onto an idealized surface. The Langmuir isotherm model is valid for monolayer sorption onto a surface containing a finite number of identical sites [17].

The sorption data were analyzed according to the linear formula of the Langmuir isotherm model (Eq.1) at 20°C. The plots of (*Ce/qe*) against equilibrium concentration (*Ce*) are shown in Fig 2. Results were found to be linear over the whole concentration range studied and the linear correlation coefficients were high. Isotherm constants a_L and K_L are presented in Table 2.

The maximum adsorption capacities, $q_{\max}$, were determined to be 93.4, 88.4 and 64 mgg^{-1} for *L. minor*, *P. crispus* and *C. vulgaris*, respectively. The plots in Fig 2 demonstrate that the Langmuir equation provides a reasonable description of the experimental data.

The low R_L value shown in Table 2 demonstrates that the adsorption behavior of biomasses were favourable (R_L <1). The low values of R_L also indicate that adsorption tends to be weakly irreversible (R_L =0).

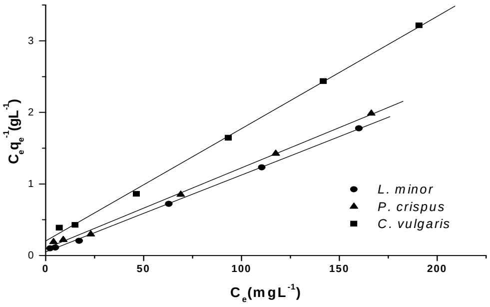

Fig. 2.Langmuir adsorption isotherms at 20 °C.

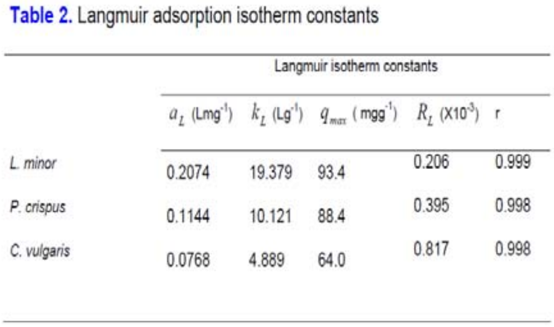

Table 2. Langmuir adsorption isotherm constants

	Langmuir isotherm constants				
	a_L (Lmg^{-1})	k_L (Lg^{-1})	q_{max} (mgg^{-1})	R_L (X10^{-3})	r
L. minor	0.2074	19.379	93.4	0.206	0.999
P. crispus	0.1144	10.121	88.4	0.395	0.998
C. vulgaris	0.0768	4.889	64.0	0.817	0.998

Adsorption Kinetics

The prediction of kinetics is necessary for the design of sorption systems. Chemical kinetics explains how fast the chemical reaction occurs and also the factors affecting the reaction rate. The nature of sorption processes depends on the physicochemical characteristics of the adsorbent as well as the system conditions. The pseudo first, pseudo second-order and intraparticle kinetic models were used to determine the adsorption kinetics. The adsorption kinetic constants, correlation coefficients and the average percentage errors between the experimental and calculated data are given in Tables 3-5. Plots of the linearised form of the pseudo first-order and pseudo second-order kinetic models are given in Figs. 3-5.

In most cases, the first-order equation of Lagergren did not apply well for the whole range of contact times but was generally applicable over the initial 20–30 minutes of the sorption process [12,18]. The calculated *qe* values of the pseudo first-order kinetics model were lower than the experimental data. Correlation coefficients of the pseudo first-order kinetics model were determined between 0.967-0.994. The sorption system for removal of Pb (II) ions by aquatic macrophyte can not be explained by pseudo first-order reaction.

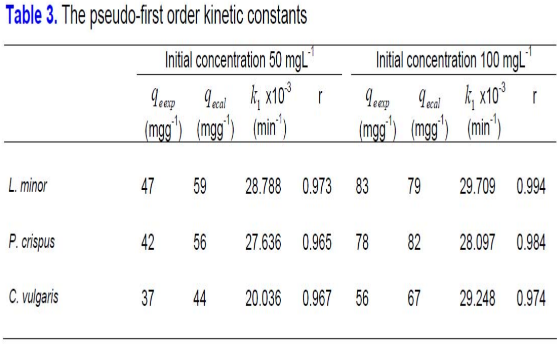

Table 3. The pseudo-first order kinetic constants

	Initial concentration 50 mgL^{-1}				Initial concentration 100 mgL^{-1}			
	q_{eexp} (mgg^{-1})	q_{ecal} (mgg^{-1})	k_1 x10^{-3} (min^{-1})	r	q_{eexp} (mgg^{-1})	q_{ecal} (mgg^{-1})	k_1 x10^{-3} (min^{-1})	r
L. minor	47	59	28.788	0.973	83	79	29.709	0.994
P. crispus	42	56	27.636	0.965	78	82	28.097	0.984
C. vulgaris	37	44	20.036	0.967	56	67	29.248	0.974

Table 4. The pseudo-second order kinetic constants

Treatment	Initial concentration 50 mgL^{-1}				Initial concentration 100 mgL^{-1}			
	q_{eexp} (mgg^{-1})	q_{ecal} (mgg^{-1})	$k_2 x10^{-3}$ (min g mg^{-1})	r	q_{eexp} (mgg^{-1})	q_{ecal} (mgg^{-1})	$k_2 x10^{-3}$ (min g mg^{-1})	r
L. minor	47	52	0.369	0.98	83	88	0.128	0.995
P. crispus	42	49	0.416	0.949	78	84	0.142	0.99
C. vulgaris	37	44	0.506	0.895	56	62	0.262	0.984

The pseudo second-order kinetic rate constant and theoretical adsorption capacity fit the experimental data and the correlation coefficients of the pseudo second-order kinetic model were higher than 0.998. This shows that the pseudo second-order adsorption mechanism was predominant for adsorption of Pb (II) ions [12].

Dried adsorbent particles have a porous structure. For this reason, the intraparticle diffusion kinetic model was applied to determine the mechanism of adsorption. The plot of q_t vs. $t^{0.5}$ demonstrated multi-linearity. This indicated the existence of intraparticular diffusion in this process. The first shape portion is the external surface adsorption stage. The second shape is the gradual adsorption stage, where the intraparticle diffusion is rate-controlled. The third shape is the final equilibrium stage. When the adsorption of the exterior surface reached saturation, the metal ions entered into the biomass particles through the pore within the particle and were adsorbed by the interior surface of the particle [19-20]. The plot of q_t vs. $t^{0.5}$ is given in Fig. 5. The initial portion represents the film diffusion. The subsequent second portion is characteristic of an intraparticular diffusion. Similar results were indicated by Ho et al., [19]. The intraparticle diffusion rate constants (k_{i1}, k_{i2} and k_{i3}) and q_e are given in Table 5. Theoretical adsorption capacity of adsorbents fit the experimental data. The order of the intraparticle diffusion rate constants were determined to be k_{i1} (first stage) $> k_{i2}$ (second stage) $> k_{i3}$ (third stage).

The intraparticle diffusion model and pseudo-second kinetic models are applicable to this adsorption system. The applicability of both models showed that the sorption process is complex and involves more than one mechanism [21].

Table 5. The intraparticle diffusion kinetic constants

Biomass	Co (mgL^{-1})	k_1 (mg $gmin^{-1}$)	r	k_2 (mg $gmin^{-1}$)	r	k_3 (mg $gmin^{-1}$)	r
L. minor	50	4.231	0.982	3.662	0.979	0.403	0.970
	100	8.537	0.943	3.267	0.931	0.337	0.902
P. crispus	50	2.756	0.999	3.435	0.971	0.134	0.999
	100	7.615	0.923	4.615	0.951	0.876	0.873
C. vulgaris	50	1.972	0.991	4.553	1.000	1.137	0.997
	100	4.952	0.889	3.820	0.994	0.538	0.931

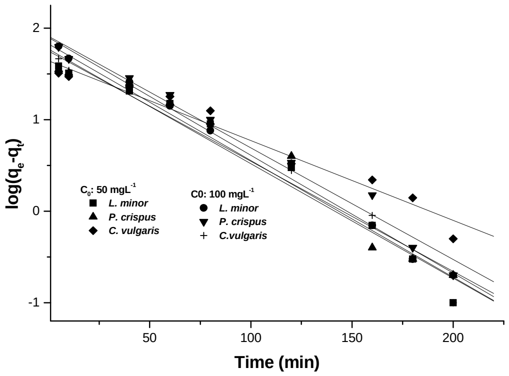

Fig. 3. Pseudo first-order adsorption kinetics

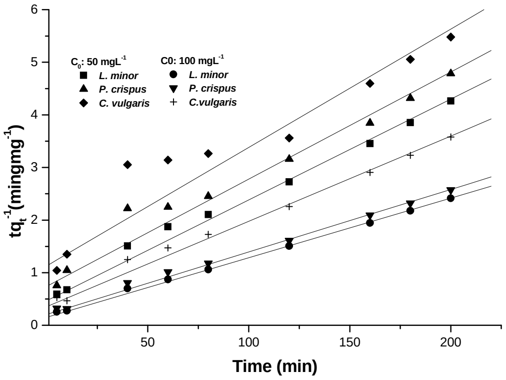

Fig. 4. Pseudo second-order adsorption kinetics

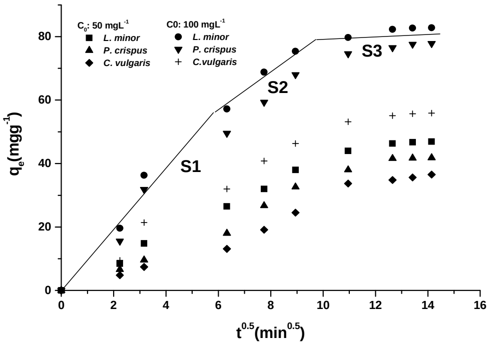

Fig. 5. Intraparticle diffusion kinetics (S1; first, S2 second and S3 third shape)

CONCLUSIONS

Adsorption of Lead ions from aqueous solution by aquatic macrophte *Lemma minor*, *Potamogeton crispus* and *Chara vulgaris* was evaluated. The Langmuir adsorption isotherm model fit very well with the studied metal concentration ranges at 20°C. The kinetics and mechanism of adsorption were determined to agree with the pseudo-second order and intraparticle diffusion kinetic models.

Optimum metal uptake capacity was determined at pH 4 for *L. minor* and *P. crispus* and pH 5 for *C. vulgaris*. Biosorption efficiency observed in the order of *L. minor* > *P. crispus* > *C. vulgaris* for removal of lead ions. The adsorption kinetics were also found to be well- described by the pseudo second-order and intra-particle diffusion models. According to FT-IR results, the biomass has different functional groups. These functional groups are able to react with metal ions in an aqueous solution. *L. minor, P. crispus* and *C. vulgaris* may be used for removal of Pb (II) ions from aqueous solution.

REFERENCES

[1] Xiangliang P, Jianlong W, Daoyong Z. 2005. Biosorption of Pb(II) by *Pleurotus ostreatus* immobilized in calcium alginate gel. Process Biochemistry. 40: 2799–2803.

[2] Saygideger S, Gulnaz O, Istifli ES, Yucel N. 2005. Adsorption of Cd(II), Cu(II) and Ni(II) ions by *Lemna minor* L.: Effect of physicochemical environment. Journal of Hazardous Materials. 126: 96-104.

[3] Majumdar SS, Das SK. Saha T, Panda, GC, Bandyopadhyoy T, Guha AK. 2008. Adsorption behavior of copper ions on *Mucor rouxii* biomass through microscopic and FTIR analysis. Colloids and Surfaces B: Biointerfaces. 63: 138–145.

[4] Gulnaz O, Saygideger S, Kusvuran E. 2005. Study of Cu (II) biosorption by dried activated sludge: effect of physico-chemical environment and kinetics study. Journal of Hazardous Materials. 120: 193-200.

[5] Romera E, Gonzalez F, Ballester A, Blazquez ML, Munoz JA. 2007. Comparative study of biosorption of heavy metals using different types of algae. Bioresource Technology. 98: 3344–3353.

[6] Ozer A, Ozer D. 2003. Comparative study of the biosorption of Pb(II), Ni(II) and Cr(VI) ions onto *S. cerevisiae*: determination of biosorption heats. Journal of Hazardous Materials. 100: 219–229.

[7] Kargi F, Cikla S. 2006. Biosorption of zinc (II) ions onto powdered waste sludge (PWS): kinetics and isotherms, Enzyme Microb Technol. 38: 705–710.

[8] Pamukoglu MY, Kargi F. 2006. Removal of copper (II) ions from aqueous medium by biosorption onto powdered waste sludge, Process Biochem. 4: 1047–1054.

[9] Langmuir I. 1918. The adsorption of gases on plane surfaces of glass, mica and platinum. J Am Chem Soc. 40: 1361–1403.

[10] Hall KR, Eagleton LC, Acrivos A, Vermeulen T. 1966. Pore and solid diffusion kinetics in fixed-bed adsorption under constant-pattern conditions. Industrial and Engineering Chemistry Fundamentals. 5: 212-223.

[11] Lagergren S. 1898. About the theory of so-called adsorption of soluble substances. K Svenska Vetenskapsakad Handl. 24: 1-39.

[12] Ho YS, McKay G. 1999. Pseudo-second order model for sorption process. Process Biochemistry. 34: 451-465.

[13] Weber WJ, Morris JC. 1963. Kinetics of adsorption on carbon from solution. Journal Sanit Engineering Dir Am Soc Cir Eng. 89: 31-60.

[14] Bux F, Kasan HC. 1994. Comparison of selected methods for relative assessment of sulfate charge on waste sludge biomass. Water SA. 20: 73–76.

[15] Goksungur Y, Uren S, Guvenc U. 2005. Biosorption of cadmium and lead ions by ethanol treated waste baker's yeast biomass, Biores Technol. 96: 103–109.

[16] Hammaini A, Gonzalez F, Ballester A, Blazquez ML, Munoz JA. 2007. Biosorption of heavy metals by activated sludge and their desorption characteristics, Journal of Environmental Management. 84: 419–426.

[17] Ng JCY, Cheung WH, McKay G. 2003. Equilibrium studies for the sorption of lead from effluents using chitosan. Chemosphere. 52: 1021–1030.

[18] Aksu Z. 2001. Equilibrium and kinetic modeling of cadmium (II) biosorption by *C. vulgaris* in a batch system: effect of temperature. Separation and Purification Technology. 21: 285–294.

[19] Ho YS, Ng JCY, McKay G. 2000. Kinetics Of Pollutant Sorption By Biosorbents: Review. Separation and Purification Methods. 29: 189–232.

[20] Wu FC, Tseng RL, Juang RS. 2001. Kinetic modeling of liquidphase adsorption of reactive dyes and metalions on chitosan. Water Research. 35: 613–618.

[21] Cheung WH, Szeto YS, McKay G. 2007. Intraparticle diffusion processes during acid dye adsorption onto chitosan. Bioresource Technology. 98: 2897–2904.